Faculty of Technology, University of Niš, Leskovac, Serbia

# Bilirubin degradation in methanol induced by continuous UV-B irradiation: a UHPLC – ESI-MS study

J. S. Stanojević, J. B. Zvezdanović, D. Z. Marković

*Received August 14, 2014, accepted October 17, 2014*

*Dejan Markovic, University of Niš, Faculty of Technology, Bulevar Oslobođenja 124, 16000 Leskovac, Serbia*
*dejan_markovic57@yahoo.com*

*Pharmazie 70: 225–230 (2015)* *doi: 10.1691/ph.2015.4122*

Degradation of bilirubin in aerobic methanol solution by continuous UV-B irradiation has been investigated in this work. The purpose of this study was to shed more light on bilirubin interaction with the UV-B component of natural sunlight, since bilirubin is a very efficient UV-B absorber located in the skin *epidermis*. The degradation products have been detected and studied by a combined method of Ultra High Performance Liquid Chromatography-Electrospray Ionization Mass Spectrometry (UHPLC-ESI-MS). Bilirubin, a toxic pigment which itself is a product of (hemoglobin) degradation in organisms, undergoes its own degradation under aerobic conditions of UV-B continuous irradiation (e.g. photooxidation) that can be partly self-sensitized. Two dipyrrolic structures have been identified as a result of the bilirubin degradation, not including the bilirubin derivative biliverdin whose increase in the irradiated system is synchronous with a time dynamics of bilirubin degradation. It appears that one of dipyrrolic products originates directly from bilirubin and biliverdin molecules, while the other one is probably connected to bilirubin self-sensitized degradation. The precursor role of biliverdin in the degradation process – related to the detected dipyrroles – has not been confirmed.

## 1. Introduction

Bilirubin (BRB) is the degradation product of the protein hemes. About 85% of bilirubin originates from hemoglobin heme, whereas the rest comes from the hemes of other proteins (myoglobin, cytochrome, catalase, peroxidase) (McDonagh 2010; Hansen 2010). The heme(s) catabolism is including heme-oxygenase action which breaks the methylene bridge between two pyrrole rings of the heme-porphyrin structure leading to formation of a green pigment, biliverdin, and its consequent conversion to a yellow pigment, bilirubin (Wang et al. 2006). Bilirubin is a toxic pigment which is transported through the bloodstream bound to albumin, so called non-conjugated BRB, liposoluble and non-excretable by the kidneys. The toxic BRB is eliminated through its ester-type linkage conjugation with glucuronic acid inside the liver hepatocytes, yielding hydrosoluble and kidney-excretable BRB-mono-(10%) and diglucuronides (90%) (Fevery 2008).

Parts of bilirubin total amount are stored in the skin *epidermis* and react with natural sunlight, including the most energetic fractions, UV-A (320-400 nm), and particularly damaging UV-B light (290-320 nm). The less energetic UV-A light penetrates deeper, in the *dermis* skin layer, because BRB and some other very important biomolecules – like flavins (riboflavin), flavonols (like quercetin), vitamins, pigments (like melanin) – present in the *epidermis* skin layer are very efficient UV-B absorbers (Wondrak et al. 2006). Both UV-A and UV-B (as the integrative parts of natural sunlight) lead to the skin photoageing effects on a larger time scale that can be accompanied by genotoxicity and cancerogenesis, mostly initiated through the (UV-absorbing) compounds photosensitizing activity following UV-absorption (Svobodova et al. 2003; Pouillot et al. 2011). That is why interaction of bilirubin with UV-light is worth of research *per se*, independent of any visible light application on BRB, and the most simple approach to get basic information is to study BRB interaction with UV-light in solution. There are few reports from the 1970's on BRB photooxidation in various solutions done with various light sources, yielding formation of different photoproducts including the ones of mono- and di-pyrolles type (Lightner and Quistad 1972a; Bonnett and Stewart 1972a; Gray et al. 1972). There are also some later reports dealing with anaerobic photoirradiation of bilirubin in solution (Itoh et al. 1999), or with aerobic and anaerobic photoirradiation of bilirubin-HSA (Human Serum Albumin) complex *in vitro* with blue-white and green light (Yasuda et al. 2001). Following this trail this work deals with BRB continuous irradiation with UV-B light in aerobic methanol solution, analysis of the yielded products by Ultra High Performance Liquid Chromatography/Electrospray Ionization Mass Spectrometry (UHPLC/ESI-MS), and elucidation of the obtained results, including consideration of existing explanative mechanisms. To our best knowledge such a study has not been done yet.

## 2. Investigations and results

Structures of bilirubin (BRB) and its derivative biliverdin (BVD), in an opened linear form, known as BRBIXα and BVDIXα, are shown in Fig. 1(A-B). As it can been seen the two tetrapyrroles have very slight structural differences: double bond in the middle of BVD structure (between the two dipyrolles entities) which does not exist in BRB structure. However, this small difference makes a huge, dramatic change in BVD absorption spectrum: the prolonged conjugation provides, besides major

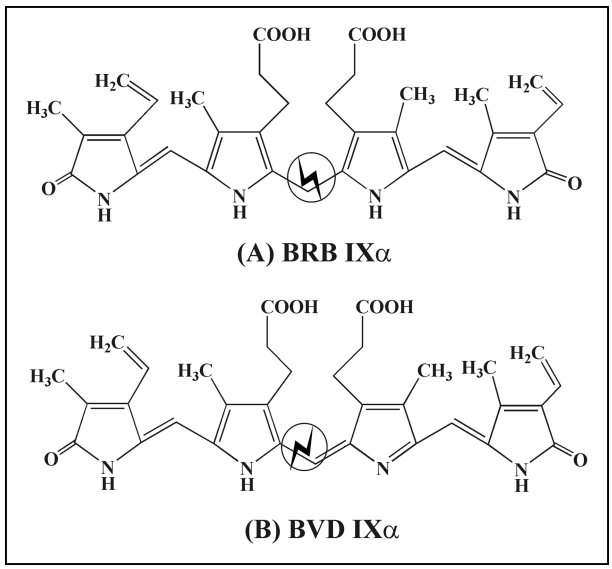


Fig. 1: Structure of bilirubin - BRBIXa isomer (A) and biliverdin -BVDIXa (B).

absorption peak now hypsochromically shifted at about 370 nm, a new minor peak with an indicative position at 660 nm (see Fig. 2B1).

The UHPLC monitored chromatograms of BRB in MeOH at $\lambda_{det.} = 405$ nm before and after 20 mins of UV-B irradiation are shown in Fig. 2A. The first two marked peaks, at the beginning of the retention scale (marked as No.1, recorded at $t_{ret.} = 1.90$ min, and No. 2, recorded at $t_{ret.} = 2.45$ min) belong to the induced products *(*Products 1 & 2, respectively). The peak No. 3 ($t_{ret.} = 3.36$ min), already existing in pre-illuminated solution, and significantly enhanced after the irradiation period, belongs to biliverdin. Finally, the major peak located at $t_{ret.} = 12.27$ min belongs to bilirubin; the two "shoulders", recorded at $t_{ret.} = 11.55$ min (left) and 13.00 min (right) belong to BRB isomers.

The absorption spectra related to BRB & BVD peaks from chromatogram shown in Fig. 2A, are shown in Fig. 2B1. The absorption spectra related to the peaks representing *Products 1 & 2* from the chromatograms in Fig. 2A, are shown in Fig. 2B2. The MS/MS spectrum of the BRB peak ($t_{ret.} = 12.27$ min) obtained in the pre-illuminated solution is shown in Fig. 3A. The most abundant fragmentation peak appeared at $m/z = 299.10$, and the anticipated structure, based on available reference data is shown in Fig. 3C (Jackson et al. 1967; Quinn et al. 2012). In addition, the MS/MS spectrum of the BVD peak ($t_{ret.} = 3.36$ min) also obtained in the pre-illuminated solution, is shown in Fig. 3B**.** Evidently, there is an obvious correspondence between MS/MS fragmentation patterns of BRB & BVD peaks, since the most abundant peak and the consequent fragment positions have been separated for two units ($m/z = 299.10$ & 271.04 in the case of BRB degradation; $m/z = 297.07$ & 269.10, in the case of BVD degradation, respectively).

The MS/MS fragmentation pattern of the peaks related to Product 1& 2 ($t_{ret.} = 1.90$ & 2.45 min, respectively) from chromatogram shown in Fig. 2A are shown in Fig. 3C&D, respectively. The proposed structures (belonging to the *Product 1& 2*) are given next to the marked protonated molecular ions in the spectra. These structures explain big difference in the absorption spectra (shown in Fig. 2B2): the additional conjugation in position 1 of the *Product* 2 (compared to the *Product 1* – Fig. 3C&D) makes huge impact in $\lambda_{max}$ shift, 292 *vs*. 405 nm, respectively.

A detected decrease of BRB concentration with the increasing periods of UV-B irradiation, obtained from a series of DAD-

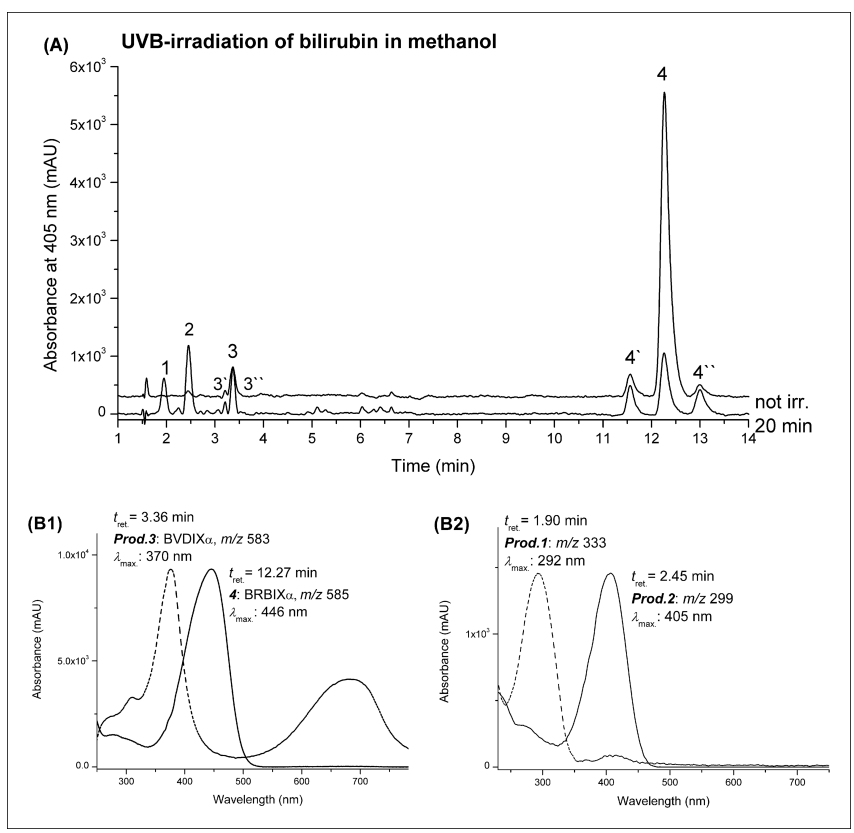


Fig. 2: Bilirubin (BRBIXa) in methanol, irradiated with continuous UV-B irradiation. The UHPLC-chromatograms for not-irradiated and 20 min irradiated BRB solution, recorded (wavelength detection) at 405 nm (A). Absorption spectra of bilirubin (peak No. 4, $t_{ret.} = 12.26$ min, from Fig. 2A: "central" BRBIXa isomer) and UVB-induced Product 3, e.g. biliverdin (BVDIXa, peak No.3, $t_{ret.} = 3.36$ min) (B1); the absorption spectra related to the peaks representing Products 1 & 2 from chromatogram shown in Fig. 2A ($t_{ret.} = 1.90$ & 2.45 min, respectively) (B2).

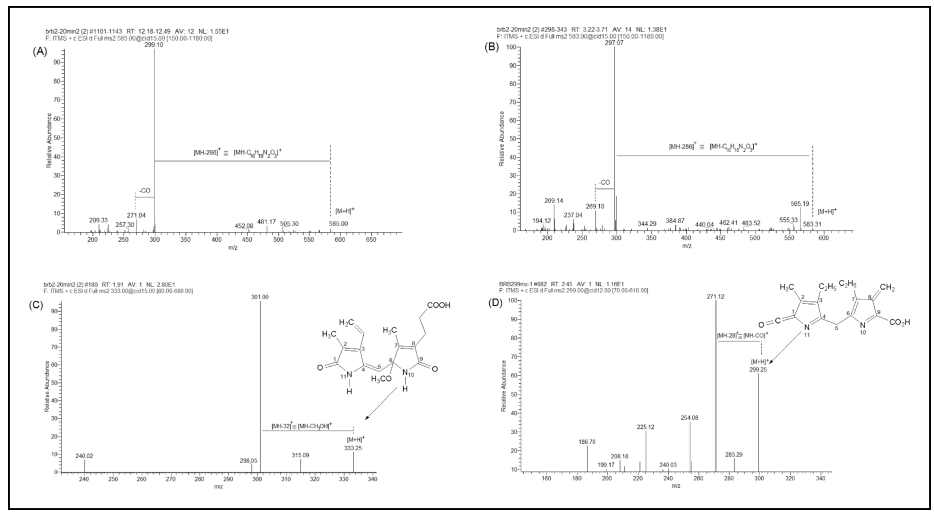

Fig. 3: The MS/MS spectra of bilirubin (peak No.4: BRBIXa, from UHPLC–chromatograms shown in Fig. 2A) (A), biliverdin (Product 3, BVDIXa, the peak No.3) (B), and the Products 1 & 2 (the peaks No.1&2) (C & D, respectively).

recorded chromatograms at 446 nm (BRB $A_{max}$), is shown in Fig. 4A. A dynamic change of BVD concentration with the increasing periods of UV-B irradiation, obtained from a series of the chromatograms at 370 nm, is shown in Fig. 4B. A detected increase of the *Product 1* concentration, obtained from a series of the chromatograms based on ESI-MS data at *m/z* 333, is shown in Fig. 4C. Finally, a dynamic change of the *Product 2* concentration with the increasing periods of UV-B irradiation, obtained from a series of the DAD-recorded chromatograms at 405 nm, is shown in Fig. 4D.

The *Product 1* is named as 2,7-dimethyl-3-vinyl-8-carboxyethyl-9-keto-6-metoxy-pyrromethenone (which corresponds to the assignment for the very similar compound made by (1983)). Accordingly, *Product 2* is named as 2-methyl-8-methylen-3,7-diethyl-1-keto-dipyrromethane-9-carboxylic acid.

Full MS spectra of the non-irradiated and irradiated samples for the given *m/z* scale (100-1000 units) have been recorded (not shown).

## 3. Discussion

Bilirubin activity is highly dependent on its conformation, having in mind that BRB has not a fixed shape. It is a flexible molecule that has different forms of stability depending on molecular environment. The shape that is dominant in crystals and solutions is a "folded form", created through intramolecular H-bonding stabilization between NH/O and OH/O groups (McDonagh and Lightner 1985). In such a structure, hydrophilic, polar -COOH and –NH groups are bound through mutual interactions and so inaccessible to the polar solvent groups, like in

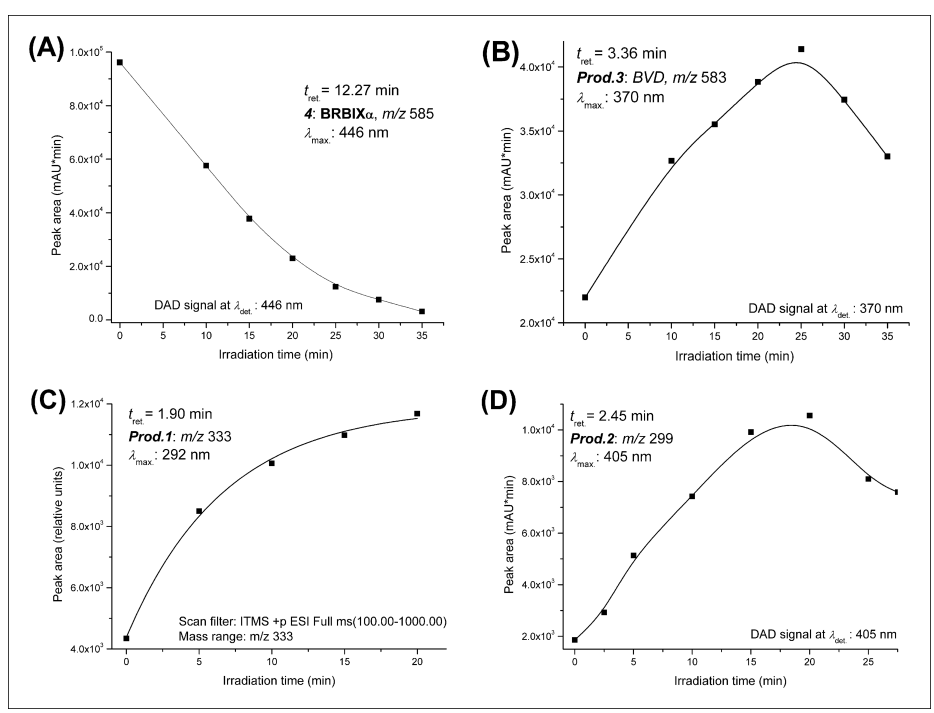


Fig. 4: The changes in peak area values for BRBIXa, BVDIXa, Products 1&2 (the peaks at $t_{ret}$.: 12.27, 3.36, 1.90 & 2.45 min, respectively, from Fig. 2A) for different irradiation time periods ($t_{irr}$.) – e.g. dynamic plots (A, B, C&D, respectively). The dynamic plots A, B&D are based on the data from DAD chromatograms at 446, 370 & 405 nm, e.g. absorption maximums for BRB, BVD & Product 2, respectively. On the other hand, the dynamic plot of Product 1 represents changes in the corresponding peak area taken from ESI-MS-data at m/z 333 (C).

water and methanol, which makes BRB less soluble in these two solvents. That is why we added $NH_4OH$, making pH more basic (pH = 8.8), allowing BRB dissolution and its transformation from a "folded" to a linear shape (Fig. 1A).

Bilirubin photooxidation in solution have been intensively investigated in the 1970 s. Thus, Lightner and Quistad (1972a) examined BRB photochemistry in oxygenated methanolic-ammonia solution irradiated for 12 h (short-term irradiation) with medium pressure mercury lamp (100 W) and observed formation of biliverdin as major product; they also isolated monopyrrole methylvinylmaleimide. In an additional study (Lightner and Quistad 1972b), by using 500W tungsten-halogen light as the source of irradiation for 36 h, they isolated and identified monopyrrole hematinic acid and two isomeric dipyrrole-type propentdyopents as methyl esters by their mass, NMR and electronic spectra. On the other hand, Bonnett and Stewart (1972a) irradiated the same sample (methanolic-ammonia solution of bilirubin) for less than 24 h with visible light (2 × 500 W) and discovered that very little biliverdin was produced, but a complex mixture of other products comprising methylvinylmaleimid (minor) and methanol-propentdyopent dipyrrole adduct (major) – in the form of one of the three possible positional isomers, characterized by its mass, NMR and electronic spectrum. All products mentioned above (among many others) appear during extended daylight irradiation (500 days) of bilirubin in chloroform (Gray et al. 1972). So, one may conclude that the use of different emitting power sources for various periods of prolonged irradiation (applied on BRB in solution) revealed not only biliverdin as the apparent product but also mono- and dipyrroles products resulting from cleavage of the original BRB molecules.

It is noteworthy to underline that yield of biliverdin obtained from BRB photooxidation depends on the solvent (more BVD is formed in chloroform than in methanol indicating a possible free radical oxidation mechanism) and BRB concentration (higher concentrations yield more BVD) (Lightner et al. 1973). Biliverdin was suggested not to be the principal precursor of BRB photoproducts formed in protic solvents as suggested thought (Gray et al. 1972), but it rather decomposes to the same products as bilirubin, including methylvinylmaleimid, hematinic acid and one of the isomeric metoxy propentdyopent (Lightner 1974; Lightner and Crandall 1972).

Following light absorption BRB undergoes non-radiative inter-system crossing from the excited singlet state, reaching the excited, longer-lived triplet state which – in the presence of oxygen – can be quenched by triplet (ground state) oxygen ($^3O_2$) producing very reactive singlet oxygen – $^1O_2$ (Lightner 1977). McDonagh (1971) has shown that BRB can sensitize its own (photo)oxidation (self-sensitation); BRB degradation rate increases in the presence of singlet oxygen sensitizers (e.g. methylene blue, Rose bengal etc.) and decreases in the presence of a singlet oxygen trap (2,5-dimethylfuran), and quenchers of singlet oxygen (e.g. β-carotene, DABCO etc.) (McDonagh 1971; Foote and Ching 1975). In other words, bilirubin is a $^1O_2$ sensitizer (in the Type II mechanism – not including free radicals (Girotti 2001)), although an inefficient one, because it can lose the photoexcitation energy by isomerization and other radiationless processes (Bonnett and Stewart 1972b; McDonagh 2011).

The following main compounds were detected in this work after continuous UV-B irradiation of bilirubin in MeOH solution (given in order of increasing retention time, $t_{ret.}$, and labeled as in Fig. 2A): *Product 1*, at *m/z* 333 ($t_{ret.}$ = 1.90 min); *Product 2*, at *m/z* 299, with a $t_{ret.}$ = 2.45 min; *Product 3*, at *m/z* 583 – three distinct isomers of biliverdin, with retention times of 3.09, 3.36 & 3.51 min (marked as peaks No.3′, 3, and 3″, respectively); and the three isomers of bilirubin eluted at 11.55, 12.27 and 13 min (peaks No.4′, 4, 4″). The MS/MS mass spectra of bilirubin and its UV-B-induced products (from chromatogram in Fig. 2A), showed the expected $[M+H]^+$ (e.g. protonated) molecular ions at *m/z* 585, 583, 333, and 299, respectively (Fig. 3A-D). The most abundant fragment ions in positive mode ESI-MS/MS spectra of different bilin pigments usually originate from fragmentation, a cleavage of the tetrapyrrole structure central position (see Fig. 1A-B), to give a prominent dipyrrole product ion (Lim 2009). In this work, protonated BRB molecular ion ($[M+H]^+$ - *m/z* 585) yields a most intense product ion at *m/z* 299 resulting from a cleavage of the central methylene bridge (Fig. 3A) – as proposed by Quinn et al. (2012) in Tandem MS experiments; the same stands for protonated biliverdin (*Prod.3*: $[M+H]^+$ - *m/z* 583) that yields most intense ion at *m/z* 297 in the analogues manner (Fig. 3B), through elimination of fragment of 286 mass units. The ions *m/z* 299 (in the case of BRB) and *m/z* 297 (in the case of BVD) were further fragmented by the loss of CO fragment (28 mass units) to give ions at *m/z* 271 and 269, respectively (Fig. 3A-B), which is in accordance with the report of Lim (2009). On the other hand, the MS/MS spectra of the *Prod.1&2* (Fig. 3C&D, respectively) showed different fragmentation patterns implicating their different structures. The MS/MS spectrum of the *Product 1* (with $[M+H]^+$ at *m/z* 333, with the proposed structure next to it (Fig. 3C) – which is one of the 4 possible cited isomers (Lightner 1977) yields a prominent fragment-ion at *m/z* 301, resulting from a loss of 32 mass units ($[MH–32]^+$ - $[MH–CH_3O–H]^+$). The *Product 2* (*m/z* 299) – with the proposed structure next to the molecular ion as shown in Fig. 3D - has been already seen in solutions of chemically degraded bilirubin with $H_2O_2$ and Fe-EDTA in the dark and aerobic conditions (De Matteis et al. 2006) and has also been described as a fragment-ion in EI-MS study done by Jackson et al. (1967); the latter authors suggested its dipyrrolic structure arising from fragmentation at the central methylene bridge, the weakest point in the BRB molecule (Fig. 1A). The MS/MS spectrum of *Prod.2* shows fragment-ions at *m/z* 271 (the loss of CO, *i.e.* 28 mass units), the *m/z* 254 peak (loss of additional 17 units - probably from OH-group), and the peak at *m/z* 225, resulting from additional loss of 29 units, which is in accordance with proposed structure (Fig. 3D).

One should add that De Matteis et al. (2006) also detected the *m/z* 333 fragment but proposed another dipyrrole type of structure. The same was done by Abu-Bakar et al. (2012) who investigated BRB metabolism by human cytochrome 450. However, neither of the two BRB studies was dealing with photoirradiation but with chemical or enzymatic oxidations.

Looking at the structure of the proposed degradation products (*1&2*) it is not possible to offer a reliable picture of the involving mechanisms. However, it looks reasonable to suppose that degradation pathway leading to *Product 1* could be probably related to BRB self-sensitized degradation *via* singlet oxygen formation: after the presumed methylene bridge cleavage *Product 1* contains two more oxygen atoms in the system (see Fig. 3C); with *Product 2* this is not the case, in the rearranged (BVD-originated) fragment there are no supporting proofs (Fig. 3D). So, it may be concluded that BRB degradation in MeOH, e.g. photooxidation, could be at least partly self-sensitized.

While the recorded MS/MS spectra were helpful for elucidation of the dipyrrolic structures of the UV-B-induced products, to get at least some more insight into mechanisms leading to dipyrrolic structures shown in Fig. 3C-D one should look to dynamic plots shown in Fig. 4A-D. The plot in Fig. 4A, obtained by integration of the chromatogram peak(s) No.4 from Fig. 2A – that belongs to the "central" BRB isomer – for different UV-B irradiation periods, clearly shows decrease of the BRB concentration with the length of irradiation in the 35 min period. The

decrease is sharp and looks linear in the first 20 min, followed by a smoother decline up to the end. When this plot is compared on the same (UV-B irradiation) time scale to dynamics plots shown in Fig. 4B, C & D, representing change of concentrations of *Prod.3, 1&2* – corresponding to the chromatogram peaks No. 3, 1 & 2 from Fig. 2A – it is evident that sharp decrease of BRB is synchronized with increase of the products concentration in the same period. The *Product 1* expresses an exponential type of rise finishing with an almost plateau point for $t_{irr.} = 20$ min (Fig. 4C); the *Product 2* shows a much sharper, linear type of rise, reaching top point in the first 20 irradiation minutes, followed by a consequent decline (Fig. 4D); finally, the *Product 3*, e.g. biliverdin, the only compound that exists in the pre-illuminated solution besides BRB itself, clearly shows the pattern very similar to the one of the *Product 2* with a small difference: the top point is now slightly shifted at $t_{irr.} = 25$ min (Fig. 4B).

Few conclusions can be drawn from this stuff and the recorded MS/MS spectra. First, it is evident that formation of the dipyrrolic *Product 1* (*m/z* 333) might be related to BRB degradation, though it has not been recorded in the BRB MS/MS spectra; otherwise it could be difficult to explain synchronicity between the two dynamic plots (Fig. 4A&C). Second, it looks undoubtful that the *Product 2* originates directly from BRB; there is direct proof in the BRB MS/MS spectrum (Fig. 3A), and the degree of synchronicity between the two dynamic plots is conceiving (Fig. 4A&D). Finally, dynamic behavior of biliverdin (shown in Fig. 4B) should put some light on BVD role during (UV-B-induced) BRB degradation. There is a report suggesting that BVD is an intermediate step (e.g. precursor) leading to monopyrrolic degradation products (Gray et al. 1972); on the other hand, there were reports in the 1970's suggesting that BVD has its own degradation pattern, leading also to the monopyrrolic and dipyrrolic degradation products, independent of the BRB degradation pathway (Lightner 1974; Lightner and Crandall 1972). At least based on the experiments done in this work, neither of these two presumptions looks conceivable. The BVD rise (Fig. 4B) could be related to BRB degradation, but it is hard to see its precursor role: the dynamic plot pattern is similar or the same as for the *Products 1&2* on the same irradiation time scale. For the same reasons it is not possible to see supporting evidence for the second presumption. Any other possible, alternative and independent BVD degradation pathway(s) cannot be postulated based on these experiments, which does not mean necessarily that it cannot emerge under at least slightly changed experimental conditions (change of UV-B intensity, UV-irradiation from the other range (for example, UV-A) combined with longer or shorter irradiation periods etc.). It should be also added that similar type of BRB-degradation products (like those obtained in this work) have also been obtained under non-irradiation conditions, using hydrogen peroxide for oxidation (Wurster et al. 2008), or diazonium salts (Kufer and Scheer 1983).

Anaerobic photodegradation of BRB has not been investigated in this work, having in mind that it would possibly imply a very different, probably a type I – sensitizing mechanism. There are reports about visible light induced appearance of geometrical *i.e.* configurational BRB photoisomers under mild irradiation conditions (Itoh et al. 1999; Yasuda et al. 2001).

At the end it is necessary to say that dipyrrole compounds similar to those found in this work have been detected in the urine of jaundiced neonates receiving phototherapy for hyperbilirubinemia (Lightner et al. 1984). The authors used HPLC chromatography for detection of the obtained products; one of the 8 detected compounds is in fact an isomer of *Product 1*. This is the proof that at least some of the obtained photoproducts were the result of photochemical degradation, e.g. photooxidation (as in this work). This is very important because phototherapy is a method of treatment of pathological jaundice that is manifested by higher BRB concentrations in the skin (Dennery et al. 2001). It consists in the application of 400-500 nm light (BRB maximal absorption range) on subcutaneous skin layers (*i.e. epidermis* which transforms toxic BRB into its conjugated hydrosoluble form (De Carvalho 2001). Phototherapy leads to a decrease of BRB in blood serum by two possible mechanisms, photoisomerization and photooxidation (de Araújo et al. 1996). The former one is faster and converts BRB into a hydrosoluble isomer, while the latter one is much slower and leads to BRB degradation. The relative contribution of the two mechanisms to BRB elimination is not known, though some *in vitro* and *in vivo* studies are prefesing photoisomerization (McDonagh and Lightner 1985). This gives a biomedical impact to the study presented in this work despite the fact that the experiments have been done in much simpler, e.g. the simplest possible system, and with much more energetic light (UV-B compared to visible light used in phototherapy). Photooxidation is reported as a minor process *in vivo*, compared to photoisomerization, but it definitely exists and the created dipyrroles are kidney-excretable (McDonagh 1985). Probably future studies with combined *in vitro* and *in vivo* research on BRB degradation, that include both UV and visible light, could possibly assemble more arguments for the mechanisms involved.

## 4. Experimental

### *4.1. Sample preparation*

A stock solution was prepared by dissolving 20 mg of bilirubin (Sigma Aldrich, Germany) in 1.5 ml of ammonium hydroxide (25%), then methanol (LC-MS grade, Baker Netherlands) was added to the final 5 ml. Bilirubin solutions were made from stock solutions freshly and stored at 4 °C until their use, protected from light with aluminum foil (to avoid any photochemical changes). The concentration of bilirubin was 0.1 mM in the final methanol solutions ready for use. All experiments were done at room temperature.

### *4.2. UV-Irradiation treatment*

Continuous UV-irradiation of the bilirubin samples in methanol (in aerobic room-conditions) was performed in a cylindrical photochemical reactor "Rayonnet", with 10 symmetrically placed lamps with emission maximum at 300 nm (UV-B). The samples were irradiated in quartz closed cuvettes (1 × 1 × 4.5 cm) placed on a rotating circular holder. The total measured energy flux was 15.0 W/m$^2$ for 300 nm lamps at 10 cm distance.

### *4.3. Ultra high performance liquid chromatography – diode array – electrospray ionization mass spectrometry analysis*

The liquid chromatography (UHPLC) runs were carried out using a Dionex Ultimate 3000 UHPLC + system equipped with a diode array (DAD) detector and also connected with LCQ Fleet Ion Trap Mass Spectrometer, Thermo Fisher Scientific, USA. The separations were performed on a Hypersil gold aQ C18 column (150 × 3 mm, 3 μm) of the same producer, at 25 °C. The small 3 μm particles have been for the first time employed for this purpose, because almost all other HPLC-MS studies dealing with BRB have been employing the bigger particles (De Matteis et al. 2006; Wurster et al. 2008; Lim 2009; Pirone et al. 2010). The mobile phase consisted of (A) 0.1% formic acid in water and (B) 0,1% formic acid in methanol. A next linear gradient program at flow rate of 0.500 ml/min has been applied: 70% to 85% (B) for first three minutes, then 85% to 100% (B) for 3$^{rd}$-4$^{th}$ min, followed by isocratic 100% (B) from 4-14 min and 100% to 70% (B) from 14-14.2 min, and finally the isocratic run with 70% (B) to 15$^{th}$ min. The injection volume was 0.7 μl.

Absorption UV-VIS spectra were recorded on a DAD-detector (with total spectral range between 200 nm and 800 nm), set at four detection wavelengths, $\lambda_{det.}$, 280 nm (for dypyrroles detection), 450 nm (close to BRB absorption maximum, $A_{max}$), 370 nm and 650 nm (BVD $A_{max}$), simultaneously. MS-Analysis was performed using a LCQ 3D-ion trap mass spectrometer with electrospray ionization (ESI) in positive ion mode. The ESI–source parameters were chosen by adjustment of those reported by Pirone et al. (2010) – who did HPLC/ESI-MS experiments on BRB extracted from a plant – and set as follows: source voltage 4.5 kV, capillary voltage 22 V, tube lens voltage 65 V, capillary temperature 250 °C, sheath and auxiliary gas flow ($N_2$) 60 and 5 (arbitrary units), respectively. MS-spectra

were obtained by full range acquisition of *m/z* 100–1000. For fragmentation study (MS/MS), a data dependent scan was performed by deploying the collision–induced dissociation (CID). The normalized collision energy of the CID cell was set at 12 and 15 eV.
All solvents used in the experiments were of HPLC or LC-MS grade. Methanol and water used in UHPLC-MS experiments (LC-MS grade) were purchased from Baker Netherlands and Fisher Scientific UK, respectively.

Acknowledgement: This work was supported under Projects of the Ministry of Education, Science and Technological development of the Republic of Serbia, Projects No.TR-34012 and OI-172044.

**References**

Abu-Bakar A, Arthur DM, Wikman AS, Rahnasto M, Juvonen RO, Vepsäläinen J, Raunio H, Ng JC, Lang MA (2012) Metabolism of bilirubin by human cytochrome P450 2A6. Toxicol Appl Pharmacol 261: 50–58.

Bonnett R, Stewart JCM (1972a) Photo-oxidation of bilirubin in hydroxylic solvents: propentdyopent adducts as major products. JCS Chem Comm 596–597.

Bonnett R, Stewart JCM (1972b) Singlet oxygen in photo-oxidation of bilirubin in hydroxylic solvents. Biochem J 130: 895–897.

de Araújo MC, Vaz FA, Ramos JL (1996) Progress in phototherapy. Sao Paulo Med J 114: 1134 –1140.

De Carvalho M (2001) Treatmant of neonatal hyperbilirubinemia. J Pediatr (Rio J) 77: S71-S80.

De Matteis F, Lord GA, Kee Lim C, Pons N (2006) Bilirubin degradation by uncoupled cytochrome P450. Comparison with a chemical oxidation system and characterization of the products by high-performance liquid chromatography/electrospray ionization mass spectrometry. Rapid Commun Mass Spectrom 20: 1209–1217.

Dennery PA, Seidman DS, Stevenson DK (2001) Neonatal hyperbilirubinemia. N Engl J Med 344: 581–590.

Fevery J (2008) Bilirubin in clinical practice: a review. Liver Int 28: 592–605.

Foote CS, Ching TY (1975) Chemistry of singlet oxygen. XXI. Kinetics of bilirubin photooxygenation. J Am Chem Soc 97: 6209–6214.

Girotti WA (2001) Photosensitized oxidation of membrane lipids: reaction pathways, cytotoxic effects, and cytoprotective mechanisms. J Photochem Photobiol B 63: 103–113.

Gray CH, Kulczycka A, Nicholson DC (1972) The photodecomposition of bilirubin and other bile pigments. JCS Perkin I 3: 288–294.

Hansen TWR (2010) Core concepts: bilirubin metabolism. Neo Rev 11: e316-e322.

Itoh S, Isobe K, Onishi S (1999) Accurate and sensitive high-performance liquid chromatographic method for geometrical and structural photoisomers of bilirubin IX alpha using the relative molar absorptivity values. J Chromatogr A 848: 169–177.

Jackson AH, Kenner GW, Budzikiewicz H, Djerassi C, Wilson JM (1967) Pyrroles and related compounds—X[1]: Mass spectrometry in structural and stereochemical problems—XC[2] Mass spectra of linear di-, tri- and tetrapyrrolic compounds. Tetrahedron 23: 603–632.

Kufer W, Scheer H (1983) The diazo reaction of bilirubin: structure of the yellow products. Tetrahedron 39: 1887–1892.

Lightner DA (1974) In vitro photooxidation products of bilirubin, in Odel GB:Schaffer R:Simopoulos AP (eds), Photherapy in the newborn: an overview, Washington, p. 34–55.

Lightner DA (1977) The photoreactivity of bilirubin and related pyrroles. Photochem Photobiol 26: 427–436.

Lightner DA, Crandall DC (1972) Biliverdin photo-oxidation. *In vitro* formation of methylvinylmaleimide. FEBS Letters 20: 53–56.

Lightner DA, Crandall DC, Gertler S, Quistad GB (1973) On the formation of biliverdin during photooxygenation of bilirubin *in vitro*. FEBS Letters 30: 309–312.

Lightner DA, Linnane WP 3rd, Ahlfors CE (1984) Bilirubin photooxidation products in the urine of jaundiced neonates receiving phototherapy. Pediatr Res 18: 696–700.

Lightner DA, Quistad GB (1972a) Methylvinylmaleimide from bilirubin photooxidation. Science 175: 324.

Lightner DA, Quistad GB (1972b) Hematinic acid and propentdyopents from bilirubin photo-oxidation *in vitro*. FEBS Letters 25: 94–96.

Lim CK (2009) High-Performance Liquid Chromotography and Mass Spectrometry of Porphyrins, Choloropylls and Bilins, Singapore, p. 208–212.

McDonagh AF (1971) The role of singlet oxygen in bilirubin photooxidation. Biochem Biophys Res Commun 44: 1306–1311.

McDonagh AF (1985) Light effects on transport and excretion of bilirubin in newborns. 453: 65–72.

McDonagh AF (2010) Controversies in bilirubin biochemistry and their clinical relevance. Semin Fetal Neonatal Med 15: 141–147.

McDonagh AF (2011) Bilirubin, copper-porphyrins, and the bronze-baby syndrome. J Pediatr 158: 160–164.

McDonagh AF, Lightner DA (1985) Like a shrivelled blood orange–bilirubin, jaundice and phototherapy. Pediatrics 75: 443–455.

Pirone C, Johnson JV, Quirke JME., Priestap HA, Lee DW (2010) Bilirubin identified in *Strelitzia reginae*, the Bird of Paradise Flower. Hort Sci 45: 1411–1415.

Pouillot A, Polla L.L., Tacchini P, Neequaye A, Polla A, Polla B (2011) Natural antioxidants and their effects on the skin, in Dayan N: Kromidas L (ed.), Formulating, Packaging, and Marketing of Natural Cosmetic Products, 1st ed., New York, p. 239–257.

Quinn KD, Nguyen NQ, Wach MM, Wood TD (2012) Tandem mass spectrometry of bilin tetrapyrroles by electrospray ionization and collision-induced dissociation. Rapid Commun Mass Spectrom 26: 1767–1775.

Svobodová A, Psotová J, Walterová D (2003) Natural phenolics in the prevention of UV-induced skin damage. A review. Biomed Papers 147: 137–145.

Wang X, Chowdhury JR, Chowdhury NR (2006) Bilirubin metabolism: applied physiology. Curr Paediatr 16: 70–74.

Wondrak GT, Jacobson MK, Jacobson EL (2006) Endogenous UVA-photosensitizers: mediators of skin photodamage and novel targets for skin photoprotection. Photochem Photobiol Sci 5: 215–237.

Wurster WL, Pyne-Geithman GJ, Peat IR, Clark JF (2008) Bilirubin oxidation products (BOXes): synthesis, stability and chemical characteristics. ActaNeurochir Suppl 104: 43–50.

Yasuda S, Itoh S, Imai T, Isobe K, Onishi S (2001) Cyclobilirubin formation by *in vitro* photoirradiation with neonatal phototherapy light. Pediatr Int 43: 270–275.